Failure Tolerance of Male and Female Lower Extremities Under Pure Bending and Combined Loading Modes

Maria Carbon, Isabella Nazari, Timothy Edinger, Jeesoo Shin, Connor Hanggi, Jason Kerrigan, and Jason Forman
Center for Applied Biomechanics, University of Virginia, United States

ABSTRACT

Lower extremity injuries remain common in frontal motor vehicle crashes, with evidence suggesting increased vulnerability among female occupants. While prior research has established failure tolerances of mid-size male lower extremities under bending and combined loading conditions, limited data exist for small female specimens. This study aimed to characterize and compare the failure tolerance of small female and mid-size male post-mortem human subject lower leg specimens under combined axial compression and posterior-anterior bending using consistent boundary conditions. Twenty-four lower leg specimens, including the tibia, fibula, and surrounding soft tissue, were obtained from 50th percentile male (n=12) and 5th percentile female (n=12) donors. Dynamic tests to failure were conducted at 1.5 m/s using a test apparatus designed to apply three-point bending in the posterior-anterior direction with varying levels of superimposed axial compression (0, 2, 4, and 6 kN). When paired left and right legs from the same donor were available, they were assigned to different loading conditions to assess the influence of axial compression magnitude. Fracture timing was determined using force, strain, acoustic emission data, high-speed video, and post-test CT imaging. Results indicated that 18 specimens fractured at the tibial shaft, 5 near the potting interface, and 1 did not fracture. Under pure bending, mean failure moments were 255 ± 57 Nm for males and 156 ± 15 Nm for females. At 6 kN axial compression, failure moments decreased to 195 Nm and 72 Nm for male and female specimens, respectively. Among matched pairs, increasing axial load resulted in an average 21% reduction in bending moment at failure. These findings demonstrate reduced failure tolerance with increasing axial compression and highlight sex-based differences. The data provides a foundation for developing improved injury risk functions and scaling methodologies for diverse occupant populations as well as informing anthropometric test devices and human body models.

INTRODUCTION

Lower extremity injuries remain one of the most common injury types in motor vehicle collisions, particularly for females (Forman et al., 2019). Traditionally, the injury risk of the lower leg, including tibia and fibula, has been estimated using the Tibia Index (TI) or the Revised Tibia Index (RTI) (Mertz 1993). These injury criteria apply the theory of normal stress in a column subjected to an eccentric axial load to predict tibia shaft fracture when the leg is subjected to combined axial compression and bending moment. The critical force and moment values for the TI were originally derived from isolated loading conditions, pure compression and pure bending. For the RTI, these critical values were updated to match new experimental results (Kuppa et al., 2001). To establish the interaction between force and moment in combined loading scenarios for application in both the TI and RTI, experiments have applied varying levels of axial compression superimposed on bending moments (reference experiments or don't say it).

This paper is a student paper from the 21st Injury Biomechanics Symposium and is published in a special issue of SAE International Journal of Transportation Safety.
It is preliminary work, has not been peer reviewed, and should not be cited because it is a work in progress.

Anthropomorphic test devices (ATDs), including the Hybrid III and Test Device for Human Occupant Restraint (THOR) families, incorporate the TI and RTI to evaluate lower-leg injury risk in crash testing. The critical values used in this formulation were derived from quasistatic experiments on mid-size male specimens and implemented for the 50th percentile male ATD. To extend this approach to other occupant sizes, including the 5th percentile female, these critical thresholds have traditionally been obtained through geometric scaling rather than direct experimental measurement. Consequently, the injury tolerance of smaller female ATDs is assumed to be a proportionally reduced version of the male response, including scaled force and moment limits. While this scaling approach provides a practical framework for injury assessment across different anthropometries, it assumes that fracture tolerance scales are predictable with body size. However, bone strength may be influenced by additional factors, including sex, age, and bone morphology (Riggs et al. 2004; Nieves et al. 2005; Schlecht et al. 2015). This limitation raises concerns regarding the validity of scaled TI parameters for female occupants and highlights the need for experimental data specific to small female specimens to improve ATD biofidelity.

Previous experimental studies have characterized the failure tolerance of mid-size male lower extremities under pure bending and/or combined loading conditions (Nyquist et al., 1985; Schreiber et al., 1997; Kerrigan et al., 2004; Ivarsson et al., 2006; Untaroiu et al., 2008). However, there remains a lack of comparable data for small female specimens tested under similar boundary conditions (Table 1). To address this gap, the present study aims to characterize the failure tolerance of both small female and mid-size male post-mortem human subject (PMHS) lower leg specimens under combined axial compression and posterior–anterior (PA) bending using consistent experimental boundary conditions.

Table 1. Lower leg studies (tibia and fibula with flesh).

Study	**Year**	**Female**	**Male**	**Loading mode**	**Loading direction**	**Loading rate (m/s)**	**Average Bending Moment (Nm)^**
Nyquist et al.	1985	4	15	Pure bending	AP, LM*	2.4-6.9	300
Schreiber et al.	1997	11	10	Pure bending / Combined loading	PA	5.5	408/311
Kerrigan et al.	2004	0	9	Pure bending	LM	1.5	262’
Ivarsson et al.	2006	6	48	Pure bending / Combined loading / Pure compression	PA, AP	1.5	252/148’

*Latero-medial bending direction.
^ Applied bending moments across all lower extremities not females versus males.
` Scaled bending moments to reference geometries (50th percentile male).

This paper is a student paper from the 21st Injury Biomechanics Symposium and is published in a special issue of SAE International Journal of Transportation Safety.
It is preliminary work, has not been peer reviewed, and should not be cited because it is a work in progress.

METHODS

Direction of loading

All tests were conducted in the posterior–anterior direction. This orientation was chosen to align with publicly available datasets, including a CIREN case review, and to enable comparison with prior work (Schreiber et al., 1997). This direction of bending is also observed in vehicle-into-barrier tests (e.g. NHTSA No. R20225387, Vehicle database No.14475), in which the THOR05F and THOR50M lower extremity load cells measured higher load frequency and peak values, respectively, further supporting its relevance to real-world impact conditions.

Anthropometry and Test Matrix

Twenty-four lower leg specimens, including the tibia, fibula, and surrounding soft tissue, were obtained from 50th percentile male (n=12) and 5th percentile female (n=12) PMHS (Table 2). Height was used as the primary selection criterion. Target heights of 151 cm for small females and 175.3 cm for average males were selected, each with an allowable variation of ±7.62 cm. This range aligns with the dimensions of the corresponding ATDs and ensures consistency with contemporary population data for small female and average male populations (Fryar et al., 2021).

This paper is a student paper from the 21st Injury Biomechanics Symposium and is published in a special issue of SAE International Journal of Transportation Safety.
It is preliminary work, has not been peer reviewed, and should not be cited because it is a work in progress.

Table 2. Donor information, including sex, age, weight, stature, and BMI.

	PMHS ID	Age	Weight (kg)	Height (cm)	BMI
Male	*901L*	72	74	177.8	23.4
	1032L	72	74	177.8	23.5
	1015L	52	74	180.3	22.7
	1034R	64	83	175.3	26.8
	1100R	45	82	182.9	24.5
	1008L	59	68	172.7	22.7
	1034L	64	83	175.3	26.8
	1008R	45	82	182.9	24.5
	1015R	52	74	180.3	22.7
	1100L	59	68	172.7	22.7
	1111R	39	82	175.3	26.6
	1116L	61	77	170.2	26.6
	Average	57	76.6	177.0	24.5
Female	*1050L*	69	40	157.5	16.3
	1105L	79	60	157.5	24.3
	1049L	69	56	152.4	24.2
	1114R	81	55	152.4	23.8
	1113R	77	49	152.4	20.9
	1120L	33	55	149.9	24.6
	1050R	69	40	157.5	16.3
	1096L	55	54	157.5	21.8
	1119L	59	36	154.9	15.1
	1120R	33	55	149.9	24.6
	1113L	77	49	152.4	20.9
	1054R	63	42	152.4	18.0
	Average	63.7	49.4	153.9	20.9

To understand the relationship between transverse load and superimposed axial compression, specimens were distributed in groups of three and tested at varying levels of superimposed axial compression: 0 kN (pure bending) and 2, 4 and 6 kN (combined loading). Additionally, when left and right legs were obtained from the same subject (n=12), the effect of the magnitude of the superimposed axial load was assessed by assigning these paired segments to distinct load conditions (Table 3).

This paper is a student paper from the 21st Injury Biomechanics Symposium and is published in a special issue of SAE International Journal of Transportation Safety.
It is preliminary work, has not been peer reviewed, and should not be cited because it is a work in progress.

Table 3. Test Matrix.

Test Condition	*PMHS ID*	*Sex*
3-point bending	*901L*	*M*
	1032L	*M*
	1015L	*M*
	1050L	*F*
	1105L	*F*
	1049L	*F*
3-point bending + 2 kN axial compression	*1034R*	*M*
	1100R	*M*
	1008L	*M*
	1114R	*F*
	1113R	*F*
	1120L	*F*
3-point bending + 4 kN axial compression	*1034L*	*M*
	1008R	*M*
	1015R	*M*
	1050R	*F*
	1096L	*F*
	1119L	*F*
3-point bending + 6 kN axial compression	*1100L*	*M*
	1111R	*M*
	1116L	*M*
	1120R	*F*
	1113L	*F*
	1054R	*F*

Specimen Preparation and Instrumentation

All PMHS were obtained and treated in accordance with the ethical guidelines established by the National Highway Traffic Safety Administration in Order 700-5, and all testing and handling procedures were reviewed and approved by the Institutional Review Board for Human Subjects Use established for the University of Virginia Center for Applied Biomechanics (Charlottesville, VA, USA). All subjects were taken for an initial CT scan to check for any bony abnormalities.

Thawed lower extremities were first disarticulated at the knee and ankle joint. Once disarticulated, the length of the lower extremity was taken from tibial spine to the tip of the medial malleolus. Around 20% of the measured length of soft tissue was removed from both the distal and proximal end of each tibia to facilitate the potting process and the adhesion of instrumentation

This paper is a student paper from the 21st Injury Biomechanics Symposium and is published in a special issue of SAE International Journal of Transportation Safety.
It is preliminary work, has not been peer reviewed, and should not be cited because it is a work in progress.

while maintaining soft tissue connectivity along the shaft. Care was taken to keep the interosseus membrane intact during the denuding, potting and testing processes. Different anthropometric measurements were taken including total specimen length and flesh circumference. Following the anthropometric measurements, the lateral malleolus (approximately 10 mm) was cut off level to the distal end of the medial malleolus to aid in the potting process.

During potting, the target alignment was to center the tibia from the center of the tibial plateau to the center of the tibial plafond (including the medial malleolus) (Figure 2a) and to maintain the definition of anterior (Figure 2b),defined by aligning the leg complex utilizing three points of contact allowing the tibia to sit on a plane (Kerrigan et al., 2004).

a)

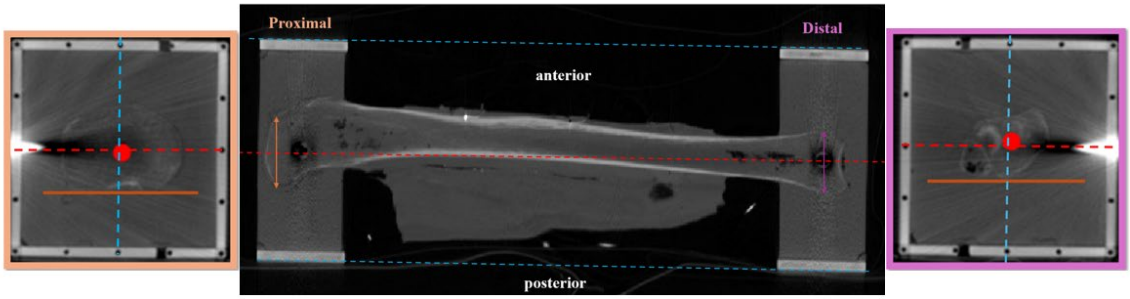

b)

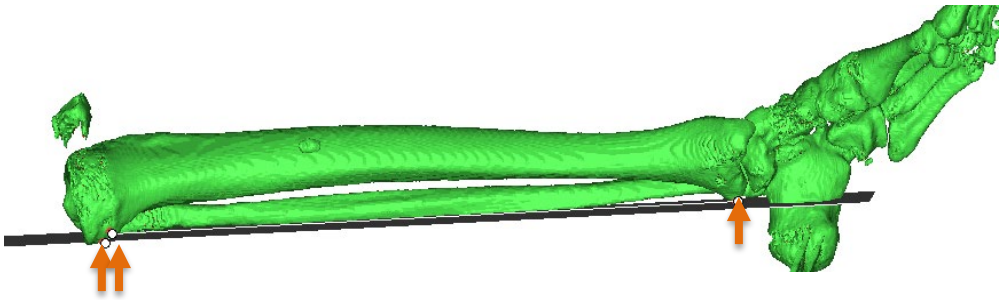

Figure 1. Example of potting alignment (a) centering targets and (b) the definition of anterior.

A custom jig was used to match this alignment with each PMHS and to maintain the length of the specimen as the total span length. Square potting cups allowed for centering, and a stage-like mechanism was used to keep the three points of contact while centering both ends of the tibia on the potting cups. The custom jig was also used to align the distal and proximal potting cups such that they were perfectly parallel to each other and perpendicular to the long axis of the tibia. The jig with the specimen was then positioned upright and the proximal potting cup filled with potting material (Smooth Cast #300, Reynolds Advanced Materials, Macungie, PA) to an approximate depth of 50 mm. When the potting material had solidified, the jig with the specimen was flipped upside down and the process repeated on the distal end.

After the specimen was potted and removed from the jig, it was instrumented with uniaxial strain gages and acoustic sensors. Strain gages were installed at a minimum of three locations on the tibia and one location on the fibula. The strain gages around the tibia were located by areas of interest for fracture and oriented to measure the strain along the longitudinal axis of the bone

This paper is a student paper from the 21st Injury Biomechanics Symposium and is published in a special issue of SAE International Journal of Transportation Safety.
It is preliminary work, has not been peer reviewed, and should not be cited because it is a work in progress.

(Untaroiu et al. 2007). Acoustic sensors were installed on both the tibia and the fibula once both ends were mounted to the test fixture, to further clarify fracture timing.

Test Fixture

Previously studied tibiofibular components (Ivarsson et al., 2006) and sectioned femurs (Ivarsson et al., 2009) were tested in a similar fixture to the one used in this study (Figure 2). The main difference was that the Ivarsson et al., 2006 study mounted the potting cups on universal joints which left all rotations unconstrained, while the present study mounted the potting cups on pin joints which permitted only in-plane rotations. The axes of rotation in the present study were at the distal and proximal ends of the specimen, while the centers of rotation in the Ivarsson et al. 2006 study were farther away from the ends of the specimen. This is because having the centers of rotation further than the specimen might have generated an induced bending moment larger than that of the eccentricity of the tibia itself. Additionally, the potting cups for this set up were modified from the Ivarsson et al., 2009 to accommodate the specimens.

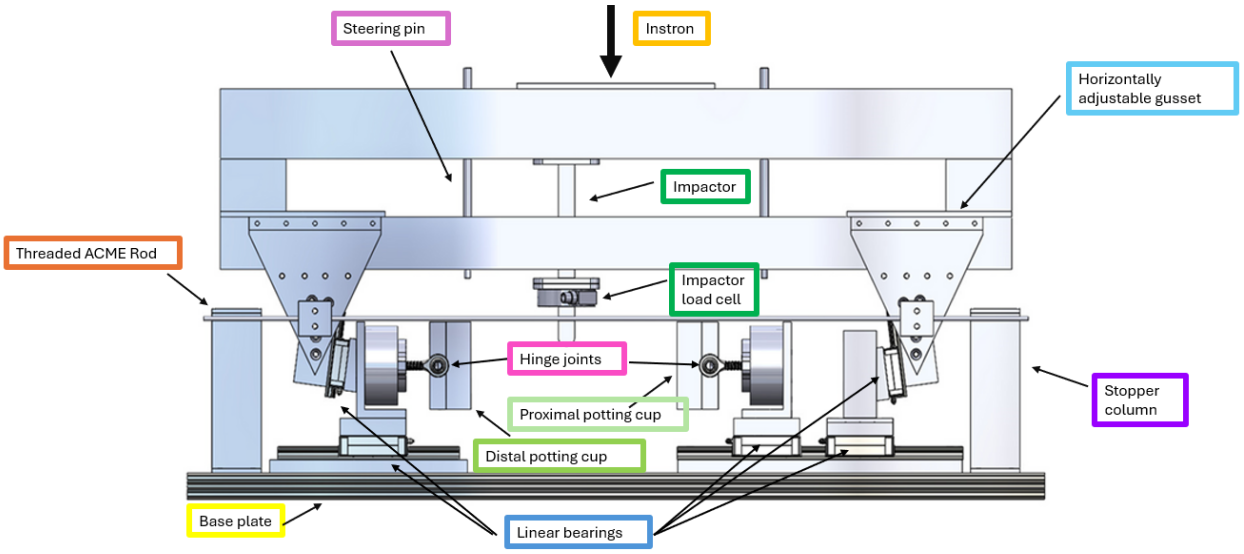

Figure 2. Test fixture components

All tests were performed in displacement control with a downward stroke of 70 mm at a speed of 1500 mm/s. For the pure bending test, a space large enough to allow the proximal slider to move freely was left between the two aluminum columns, and the two aluminum blocks in between the upper and lower horizontal beam are removed such that the upper horizontal beam with the impactor could move independently while the lower horizontal beam stayed in place (Figure 3). This allowed for a free boundary on the proximal side and a fixed boundary on the distal side.

This paper is a student paper from the 21st Injury Biomechanics Symposium and is published in a special issue of SAE International Journal of Transportation Safety.
It is preliminary work, has not been peer reviewed, and should not be cited because it is a work in progress.

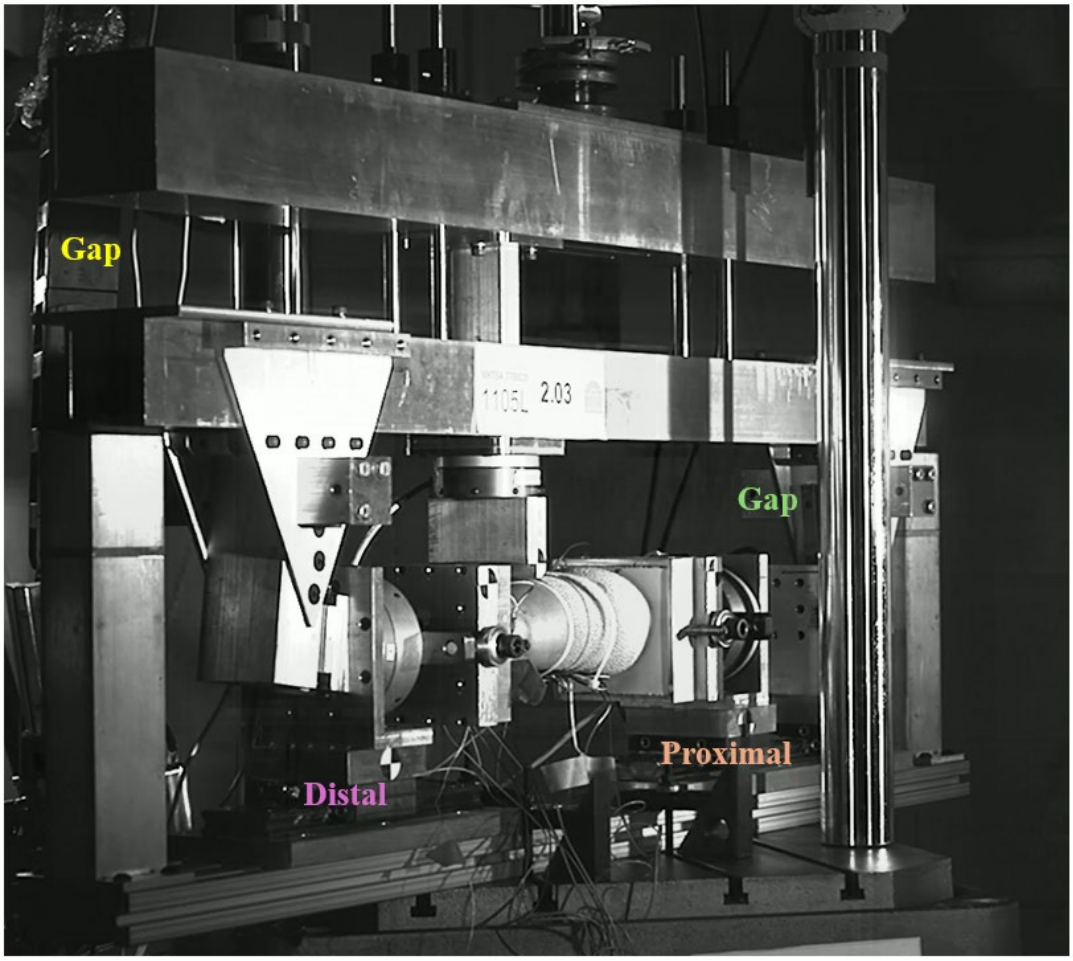

Figure 3. Test fixture set up for pure bending.

In combined loading, a 120-psi crush-strength honeycomb (Plascore Aluminum Honeycomb) was sized by area to act as an axial compression load limiter. The honeycomb piece was placed between the two aluminum columns (Figure 4), and the gusset was moved to create a 50-150 N compressive preload on the distal load cell. When the actuator with the upper part of the set-up moved downward, the aluminum columns on the horizontal linear bearings were forced inwards causing axial compression in the specimen. Due to the geometrical constraint imposed by the set-up, the specimen was axially compressed at a ratio of $2 \cdot \tan(7.5°) = 0.263$ mm per millimeter of downwards actuator displacement (Figure 4). The honeycomb maintained a constant force limit equal to the load capacity of the honeycomb. After approximately 15-30 mm of downwards actuator displacement, the impactor contacted the axially preloaded specimen and caused it to fail in three-point bending. The axial compression force created a relatively large moment where the triangular gussets are cantilevered to the lower horizontal beam. To reduce this moment and thus prevent damage to the set-up, the right and left gussets were connected by threaded rods.

This paper is a student paper from the 21st Injury Biomechanics Symposium and is published in a special issue of SAE International Journal of Transportation Safety.
It is preliminary work, has not been peer reviewed, and should not be cited because it is a work in progress.

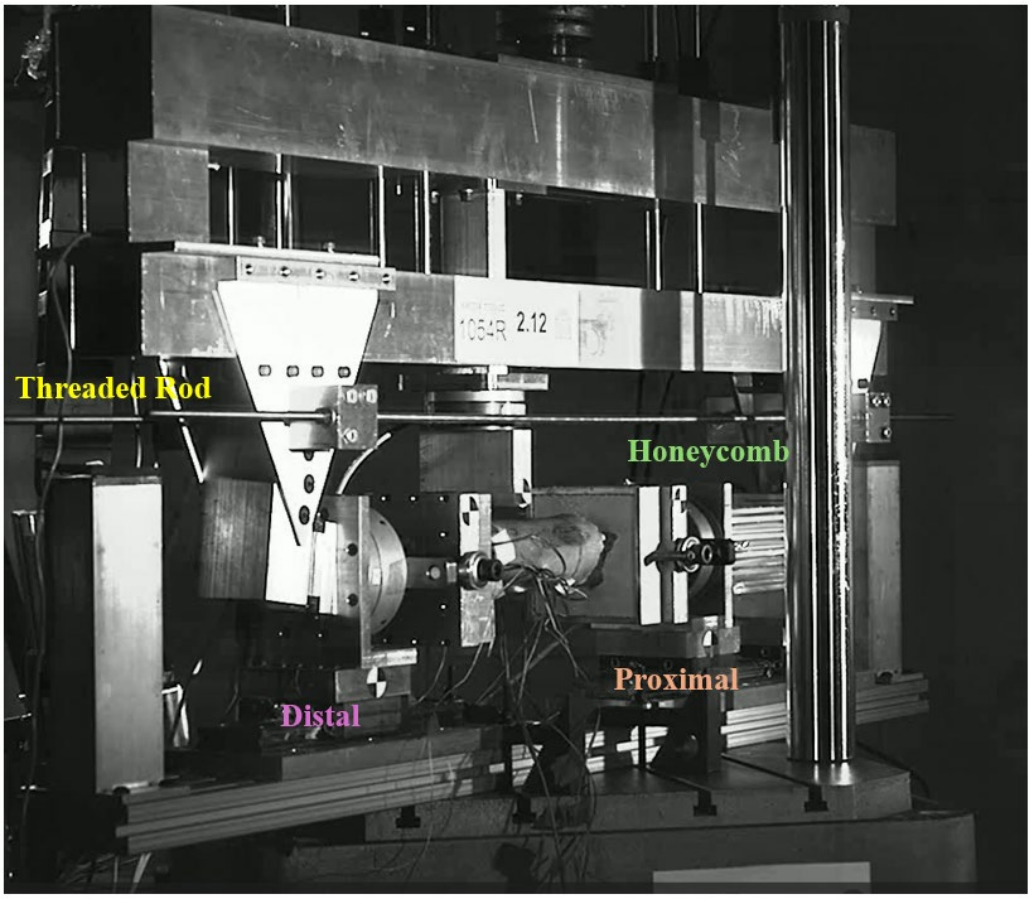

Figure 4. Test fixture set up for combined loading.

Data Analysis and Injury Identification

Two independent sources were used to obtain the load time history of the three-point bending force in the pure bending and combined loading tests: 1) the impactor load cell and 2) the sum of the recorded vertical forces recorded by the distal and proximal six axis load cells. For all tests, the force-time history measured by the impactor load cell was inertially compensated. The time history of three-point bending force was determined from the distal and proximal side six axis load cells. Failure occurred a few milliseconds after the drastic reduction in bone strain and at a slightly higher level of force than indicated by the signal from the impactor load cell (Figure 3a and 3b). In contrast, failure according to the signal from the impactor load cell always coincided exactly with the drastic reduction in bone strain, suggesting that the impactor load cell gives a more accurate estimate of the true three-point bending force than the signals from distal and proximal side six axis load cells and consequently, that the bending moment in the specimen due to three-point bending should be determined from the compensated impactor load cell signal.

The bending moment induced in the specimen by the three-point bending load reached its maximum at the point of impactor contact and decreased linearly to zero at the centers of rotation of the right and left hinge joints. Because the tibiofibular complex was loaded at the distal third of

This paper is a student paper from the 21st Injury Biomechanics Symposium and is published in a special issue of SAE International Journal of Transportation Safety.
It is preliminary work, has not been peer reviewed, and should not be cited because it is a work in progress.

the total span, and all observed fractures occurred within this region or closer to the distal end, the external bending moment was calculated as follows:

$$M_{ext} = F_{ext}(L - x)(\frac{x}{L})$$

where M_{ext} is the external moment, F_{ext} is the impactor load, x is the distance from the center of rotation of the left side hinge to the impactor location and one third of the span, and L is the span length which equals the distance between the hinge joints that are in fact the centers of rotation of the system (Figure 5).

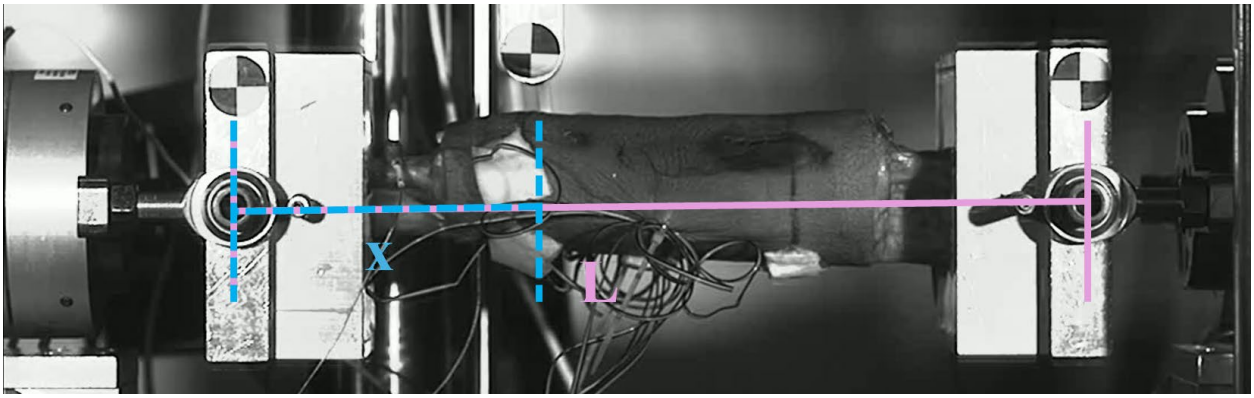

Figure 5. Diagram of distances used to calculate bending moment.

In-depth analysis of acoustic sensor signals, strain gage responses, force data, high-speed video, and pre-test versus post-test CT scans were used to determine the timing and type of injury following previous published work (Tushak et al., 2022). Four primary indicators of specimen failure were identified from the time histories: (1) peak bending load in the pure bending and combined loading tests, (2) initiation of rapid strain reduction (Figure 3c and 3d), (3) a spike in the acoustic signal (Figure 3e and 3f), and (4) initiation of rapid load reduction, corresponding to structural collapse. In nearly all the combined loading and pure bending tests, these phenomena occurred simultaneously and thus indicated consistent levels of axial compression force and three-point bending load at the point of failure. In the few cases where they did not coincide exactly, the different indicators still produced similar values for axial compression and/or bending force at failure.

This paper is a student paper from the 21st Injury Biomechanics Symposium and is published in a special issue of SAE International Journal of Transportation Safety.
It is preliminary work, has not been peer reviewed, and should not be cited because it is a work in progress.

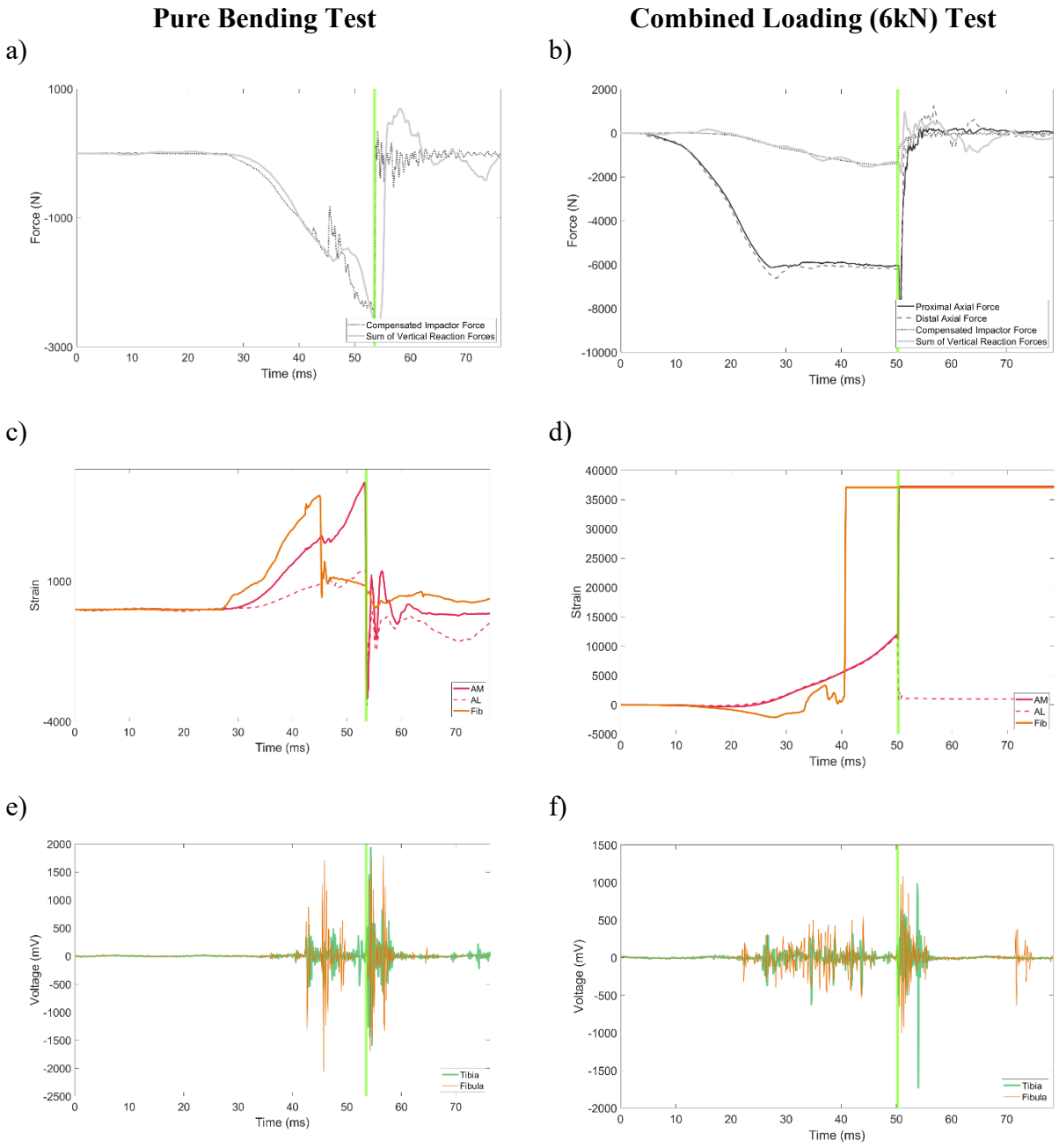

Figure 6. Example data for injury timing determination, including forces(a, b), microstrain in the anterior tibia and fibula locations (c, d), and acoustic signal for the tibia and the fibula (e, f). Timing of tibia fracture is noted by a green vertical line. Strain gage locations are anteromedial (AM), anterolateral (AL) and fibula (Fib).

RESULTS

Of the 24 lower leg specimens, 18 failed at the tibial shaft, 5 failed near/at the potting interface, and 1 tibia did not fracture (Table 3). Under the highest compressive load (6kN), three

This paper is a student paper from the 21st Injury Biomechanics Symposium and is published in a special issue of SAE International Journal of Transportation Safety.
It is preliminary work, has not been peer reviewed, and should not be cited because it is a work in progress.

tibiae displayed complex/comminuted fractures with respect to the rest of the data set. Seventeen lower legs displayed sequential fracture spikes (10 male, 7 female), indicating fibula fracture before tibia fracture, while the rest had a singular spike in force (2 male, 5 female), which indicate a simultaneous fracture or fracture away from the point of impactor contact.

Table 4. AIS15 Code, compression force and external force at failure and fracture location

Test Condition	PMHS ID	Sex	AIS2015 Code	Compression Force (N)	External Moment (Nm)	Fracture location
3-point bending	901L	M	854251.2	0	335	Shaft
	1032L	M	854251.2	0	203	Shaft
	1015L	M	854251.2	0	228	Shaft
	1050L	F	854261.2	0	156	Shaft
	1105L	F	854251.2	0	138	Shaft
	1049L	F	854251.2	0	174	Shaft
3-point bending + 2 kN axial compression	1034R	M	854251.2	1596	265	Shaft
	1100R	M	854251.2	1602	243	Shaft
	1008L	M	854251.2	2193	377	Shaft
	1114R	F	854261.2	1837	133	Near distal interface
	1113R	F	854251.2	1817	133	Near distal interface
	1120L	F	854251.2	1221	149	Shaft
3-point bending + 4 kN axial compression	1034L	M	854261.2	4168	234	Shaft
	1008R	M	854261.2	3096	277	Shaft
	1015R	M	854251.2	3761	210	Near distal interface
	1050R	F	854261.2	3630	113	Shaft
	1096L	F	854251.2	3948	138	Shaft
	1119L	F	854261.2	4042	76	Near distal interface
3-point bending + 6 kN axial compression	1100L	M	854271.2	6207	181	Shaft
	1111R	M	No tibia injury	-	-	Did not fracture
	1116L	M	854261.2	6219	208	Shaft
	1120R	F	854271.2	6034	105	Shaft
	1113L	F	854251.2	5436	0	At potting interface
	1054R	F	854271.2	6163	39	Shaft

This paper is a student paper from the 21st Injury Biomechanics Symposium and is published in a special issue of SAE International Journal of Transportation Safety.
It is preliminary work, has not been peer reviewed, and should not be cited because it is a work in progress.

Among the matched pairs tested, female subject 1050 exhibited a substantial difference in failure moment. The left leg failed at 156 Nm under pure bending, whereas the right leg failed at 113 Nm under combined loading (4 kN), resulting in a 43 Nm difference. Other matched pairs subjected to the same difference in superimposed axial load also showed notable left–right differences in failure moment. Specifically, male subject 1100 (left/right) failed at 181 Nm and 243 Nm, respectively, corresponding to a larger difference of 62 Nm.

Average external moment for males and females varied by loading mode (Table 5). Under three -point PA bending, average failure moments were 255 Nm for males and 156 Nm for females. With the addition of 2 kN superimposed axial compression, average failure moments were 295 Nm for males and 138 Nm for females. Under 4 kN axial compression, average failure moments were 240 Nm for males and 109 Nm for females. Finally, with 6 kN axial compression, average failure moments were 195 Nm for males and 48 Nm for females. Overall, failure moments were consistently higher in males than females across all loading modes, while variability in females increased with higher axial compression levels.

Table 5. Mean, range, and standard deviation for male and female lower legs.

Loading Condition	Males Mean (Nm)	Range (Nm)	SD (Nm)	Females Mean (Nm)	Range (Nm)	SD (Nm)
3-point bending	255	203–335	70	156	138–174	18
2 kN axial compression	295	243–377	70	138	133–149	9
4 kN axial compression	240	210–277	34	109	76–138	31
6 kN axial compression	195	181–208	19	48	0–105	54

DISCUSSION

The goal of this study was to quantify the failure tolerance of female and male lower legs under pure bending and combined loading modes. At the time of failure, axial compression force was recorded, and the transverse load was used to compute the external bending moment values.

Eighteen of the 24 tested lower legs sustained clinically relevant fractures that resembled those reported in field studies (Ivarsson et al., 2006). Five failures occurred at the potted boundary and likely represented an underestimation of the failure tolerance, forces, and moments of the lower leg. Fractures in this second group may have been artificial due to the stiff potting resin boundary condition and stress concentrations caused by the screws used to improve potting grip. However, one lower leg (1111R) did not exhibit any sign of tibia failure, while the fibula did

This paper is a student paper from the 21st Injury Biomechanics Symposium and is published in a special issue of SAE International Journal of Transportation Safety.
It is preliminary work, has not been peer reviewed, and should not be cited because it is a work in progress.

fracture. This could indicate that tibia stiffness is highly variable among individuals and could vary based on several parameters.

The “fibula effect”, reported by Kerrigan et al., 2004 and seen in Schreiber et al., 1997, was observed in 17 of the 24 tests performed in this study, and it is the effect the fibula has characterized by an abrupt decrease in reaction force and thus bending moment. The presence of twin peaks in the impactor load is attributed to the failure of the fibula while the lower leg is being loaded. Forces are higher than those observed to the fibula loaded alone and could be attributed to the tibia being loaded simultaneously at the time of fibula failure. This can be observed using the strain data of the tibia at the time of fibula failure. The “fibula effect” can also contribute to fracture timing and tolerance of the lower leg complex. In posterior–anterior loading and the lateromedial loading, the fibula is in direct path of the impactor, whereas in the anterior posterior and mediolateral bending direction the tibia is being loaded first. In some cases, the fibula does not fracture as observed by Ivarsson et al., 2006. In this case, twin peaks are not present, and the fracture tolerance can be attributed to just the tibia fracture.

Matched pairs tested did exhibit differences in applied bending moment at the time of failure when superimposed axial compression force was increased. Compared to Schreiber et al., who studied the differences between bending and a single level of superimposed axial load (4kN), the differences seem to vary across match pairs with no fixed percentage of bending moment decrease. For this study a 21% decrease in bending moment was observed, yet not all matched pairs were tested across the same initial and final conditions because they were allocated to different parts of the test matrix. Future work should include matched pairs being tested at the same levels for a more robust conclusion.

Across the different loading modes, clear differences appear between male and female specimens in both the range and distribution of external moments at failure. Overall, male lower legs failed under higher transverse loads than females at all superimposed axial loads. Contributing factors to differences in failure tolerance can be total span length, with males having a generally higher span length than females as well as cross sectional areas, due to the select anthropometries. Female lower legs did experience a substantial decrease in transverse load and thus bending moment needed for failure at the highest superimposed axial load with one lower leg failing in pure compression.

CONCLUSIONS

This study characterized the failure tolerance of small female and mid-size male PMHS leg specimens under pure bending and combined loading conditions. Male lower legs consistently exhibited higher failure moments than female lower legs across all loading modes, indicating greater overall bending tolerance. Increasing axial compression generally reduced bending moment at failure, with an observed average decrease of about 21%, although this effect varied across specimens and matched pairs. Additionally, the “fibula effect” was frequently observed and influenced failure behavior, highlighting the complex interaction between the tibia and fibula in determining fracture timing and tolerance. These data can not only be compared to pre-existing data sets to provide a more comprehensive insight into the failure tolerance of the leg for both mid-size males and small females but also be leveraged to develop injury risk functions for the leg

This paper is a student paper from the 21st Injury Biomechanics Symposium and is published in a special issue of SAE International Journal of Transportation Safety.
It is preliminary work, has not been peer reviewed, and should not be cited because it is a work in progress.

complex. Additionally, it can be used to inform forces and moments measured by the ATDs and further validate HBMs. Future work includes the use of scaling techniques to normalize the data set and subsequently scale the response across varying anthropometries.

ACKNOWLEDGEMENTS

The authors would like to acknowledge the National Highway and Traffic Safety Administration (NHTSA) for financial support of this research. It should be noted that the views or opinions expressed here are those of the authors and not necessarily aligned with the views and opinions of the sponsoring organization.

REFERENCES

Forman, F., Poplin, G. S., Shaw, C. G., McMurry, T. L., Schmidt, K., Ash, J., & Sunnevang, C. (2019). Automobile injury trends in the contemporary fleet: Belted occupants in frontal collisions. Traffic Injury Prevention, 20(6), 607–612. https://doi.org/10.1080/15389588.2019.1630825

Fryar, C. D., Carroll, M. D., Gu, Q., Afful, J., & Ogden, C. L. (2021). Anthropometric reference data for children and adults: United States, 2015–2018 (Vital and Health Statistics Series 3, No. 46). National Center for Health Statistics.

Ivarsson, B. J., Genovese, D., Crandall, J. R., Bolton, J. R., Untaroiu, C. D., & Bose, D. (2009). The tolerance of the femoral shaft in combined axial compression and bending loading (SAE Technical Paper No. 2009-22-0010). https://doi.org/10.4271/2009-22-0010

Kerrigan, J. R., Drinkwater, D. C., Kam, C. Y., Murphy, D. B., Ivarsson, B. J., Crandall, J. R., & Patrie, J. (2004). Tolerance of the human leg and thigh in dynamic latero-medial bending. International Journal of Crashworthiness, 9(6), 607–623. https://doi.org/10.1533/ijcr.2004.0315

Mertz, H. J. (1993). Anthropometric test devices. In A. M. Nahum & J. W. Melvin (Eds.), Accidental injury: Biomechanics and prevention. Springer-Verlag.

Nieves, J. W., Formica, C., Ruffing, J., Zion, M., Garrett, P., Lindsay, R., & Cosman, F. (2005). Males have larger skeletal size and bone mass than females, despite comparable body size. Journal of Bone and Mineral Research, 20(3), 529–535. https://doi.org/10.1359/JBMR.041005

Nyquist, G. W., Cheng, R., El-Bohy, A. A., & King, A. I. (1985). Tibia bending: Strength and response. SAE Transactions, 94, 240–253.

Riggs, B. L., Melton, L. J., Robb, R. A., Camp, J. J., Atkinson, E. J., Peterson, J. M., Rouleau, P. A., McCollough, C. H., Bouxsein, M. L., & Khosla, S. (2004). Population-based study of age and sex differences in bone volumetric density, size, geometry, and structure at different skeletal sites. Journal of Bone and Mineral Research, 19(12), 1945–1954. https://doi.org/10.1359/JBMR.040916

Schlecht, S. H., Bigelow, E. M., & Jepsen, K. J. (2015). How does bone strength compare across sex, site, and ethnicity? Clinical Orthopaedics and Related Research, 473(8), 2540–2547. https://doi.org/10.1007/s11999-015-4253-4

Schreiber, P., Crandall, J., Hurwitz, S., & Nusholtz, G. S. (1998). Static and dynamic bending strength of the leg. International Journal of Crashworthiness, 3(3), 295–308. https://doi.org/10.1533/cras.1998.0077

Tushak, S. K., Donlon, J. P., Gepner, B. D., Chebbi, A., Pipkorn, B., Hallman, J. J., Forman, J. L., & Kerrigan, J. R. (2022). Failure tolerance of the human lumbar spine in dynamic combined compression and flexion loading. Journal of Biomechanics, 135, 111051. https://doi.org/10.1016/j.jbiomech.2022.111051

This paper is a student paper from the 21st Injury Biomechanics Symposium and is published in a special issue of SAE International Journal of Transportation Safety.
It is preliminary work, has not been peer reviewed, and should not be cited because it is a work in progress.

Untaroiu, C., Ivarsson, J., Genovese, D., Bose, D., & Crandall, J. (2008). Biomechanical injury response of leg subjected to combined axial compressive and bending loading. Stapp Car Crash Journal, 52, 351–374.